energies

MDPI

Article

Highly Efficient 3rd Generation Multi-Junction Solar Cells Using Silicon Heterojunction and Perovskite Tandem: Prospective Life Cycle Environmental Impacts

René Itten * and Matthias Stucki

Institute of Natural Resource Sciences, Zurich University of Applied Sciences, 8820 Wädenswil, Switzerland; matthias.stucki@zhaw.ch

* Correspondence: rene.itten @zhaw.ch; Tel.: +41-58-934-52-322

Academic Editor: Jean-Michel Nunzi

Received: 31 May 2017; Accepted: 14 June 2017; Published: 23 June 2017

Abstract: In this study, the environmental impacts of monolithic silicon heterojunction organometallic perovskite tandem cells (SHJ-PSC) and single junction organometallic perovskite solar cells (PSC) are compared with the impacts of crystalline silicon based solar cells using a prospective life cycle assessment with a time horizon of 2025. This approach provides a result range depending on key parameters like efficiency, wafer thickness, kerf loss, lifetime, and degradation, which are appropriate for the comparison of these different solar cell types with different maturity levels. The life cycle environmental impacts of SHJ-PSC and PSC solar cells are similar or lower compared to conventional crystalline silicon solar cells, given comparable lifetimes, with the exception of mineral and fossil resource depletion. A PSC single-junction cell with 20% efficiency has to exceed a lifetime of 24 years with less than 3% degradation per year in order to be competitive with the crystalline silicon single-junction cells. If the installed PV capacity has to be maximised with only limited surface area available, the SHJ-PSC tandem is preferable to the PSC single-junction because their environmental impacts are similar, but the surface area requirement of SHJ-PSC tandems is only 70% or lower compared to PSC single-junction cells. The SHJ-PSC and PSC cells have to be embedded in proper encapsulation to maximise the stability of the PSC layer as well as handled and disposed of correctly to minimise the potential toxicity impacts of the heavy metals used in the PSC layer.

Keywords: life cycle assessment (LCA); photovoltaics; perovskite; multi-junction; tandem; silicon heterojunction; greenhouse gas; carbon footprint; electricity

1. Introduction

The global energy demand of industry and households is responsible for more than 50% of the global greenhouse gas emissions [1] and continues to increase [2]. Photovoltaic (PV) solar energy conversion can support the transition from fossil fuels to more sustainable energy generation and reduce global greenhouse gas emissions significantly. However, photovoltaic technology is still evolving rapidly, not only for the emerging third generation PV technologies like organic solar cells (OPV), dye-sensitised solar cells (DSSC), and perovskite (PSC) solar cells, but also for the more mature technologies like second generation copper-indium-gallium-selenide (CIGS) and cadmium-telluride (CdTe) solar cells and the first generation crystalline silicon-based (CS) solar cells.

A promising new technology for the highly efficient generation of photovoltaic electricity is silicon heterojunction (SHJ) solar cells. De Wolf et al. [3] performed an extensive review of SHJ cells and concluded that this cell type is viable for industrial production due to its high efficiency, simple processing, and high temperature stability, in addition to the use of thinner wafers. Louwen et al. [4]

performed a prospective life cycle assessment of SHJ solar cells and identified the potential of SHJ cells to reduce the life cycle environmental impacts of photovoltaic electricity compared to mono-crystalline silicon cells.

Another promising technology for cost efficient solar electricity generation is perovskite solar cells (PSC), which, according to Snaith [5], are currently limited mostly by stability. However, recent results published in late 2016 and early 2017 [6–13] show promising improvements of PSC cell stability if the PSC layer is combined with inorganic hole and electron transport layers or the replacement of organic with inorganic cations. Gong et al. [14], Espinosa et al. [15], and Serrano-Lujan et al. [16] applied life cycle assessment (LCA) methodology to PSC for laboratory scale production. Celik [17] performed an LCA for scaled production of PSC from lab to fab. They all determined that the electricity demand of the various deposition processes and the stability as well as the lifetime of PSC are crucial in order for it to be competitive with first and second-generation solar cells.

PSC can be combined with first and second generation solar cells in either monolithic 2-terminal or stacked 4-terminal tandem solar cells with high efficiency [9–12,18–25]. The combination of the SHJ and PSC technologies in multi-junction tandem cells has the potential to achieve a conversion efficiency of up to 30%, significantly reducing the area required for photovoltaic electricity generation [26]. Espinosa and Krebs [27] compared the environmental impacts of organic single-junction and tandem cells. They revealed that a relative increase in efficiency of more than 20% is necessary in order for the tandem cell to perform better than the single-junction. Monteiro-Lunardi et al. [28] combined the results of Espinosa et al. [15] and Louwen et al. [4] to perform a LCA of SHJ-PSC tandem cells based on laboratory data for perovskite production. They concluded that the use of aluminium instead of silver or gold for the electrodes as well as the avoidance of organic hole and electron transport materials will reduce the environmental impacts of tandem cells.

This study aims to compare the future environmental impacts of crystalline silicon based PV modules with single junction PSC cells and monolithic SHJ-PSC tandem cells with a prospective LCA. The prospective assessment of crystalline silicon cells is based on future predictions for key parameters of the photovoltaic cells according to the International Technology Roadmap for Photovoltaics (ITRPV). In addition, the cell structure of the monolithic SHJ-PSC tandem cells and the PSC single junction cells are adjusted to prospective industrial production processes using an industrial production design relying on scalable deposition processes and inorganic hole and electron transport layers for improved stability. The industrial production designs of single-junction perovskite and monolithic 2-terminal tandem cells are based on recent published literature in late 2016 and early 2017 [9–12,25].

The model approach applied in this paper combines future predictions for key parameters of the photovoltaic supply chain with parametrised life cycle inventory for all cell types in order to enable an appropriate comparison of photovoltaic technologies with different levels of maturity. This prospective approach results in a range of different future results similar to the approaches in Louwen et al. [4], Celik et al. [17], Frischknecht et al. [29], and Rufer and Braunschweig [30]. Furthermore, the comparison does not only include mono-crystalline but also poly-crystalline silicon cells, which currently cause similar or lower environmental impacts than the mono-Si [31], as future reference for the PSC single-junction and the SHJ-PSC tandem cells.

2. Materials and Methods

2.1. Goal and Scope

The goal of this study was the quantification of relevant environmental impacts of monolithic 2-terminal SHJ-PSC tandem cells, as well as those of PSC solar cells. In addition, the environmental impacts of these two cell types were compared with current and future competing crystalline silicon-based solar cells by means of a prospective Life Cycle Assessment (LCA) with a time horizon of 2025. The Life Cycle Inventory (LCI) data were based on primary data on the structure of novel photovoltaic cells obtained from recent literature published in late 2016 and early 2017 [9–12].

2.2. Functional Unit and System Boundaries

The functional unit in this study is 1 kWh low voltage AC electricity delivered to the electricity network, following the recommended functional unit for the comparison of different photovoltaic technologies according to the International Energy Agency Photovoltaic Power Systems Programme (IEA-PVPS) methodology guidelines on LCAs of photovoltaic electricity [32]. A schematic representation of the production system under study is shown in Figure 1. The system for the SHJ and PSC solar electricity generation includes raw material extraction, energy supply and its associated energy use, crystalline silicon production, the mounting system including the aluminium supply chain, and the production of inverters and electrical equipment, as well as cell and module production. The inventories include all relevant material and energy flows as well as onsite emissions and treatment of waste air. Furthermore, module transport to the site of the power plant and maintenance during the operation of the power plant (including the replacement of damaged modules and cleaning of the power plant) are included. The system boundaries comply with the recommendations of the IEA-PVPS [32]. The system is divided into fore- and background systems. The raw material and energy supply chains are part of the background system, whereas the production of the PSC solar cells and the SHJ-PSC tandem cells, as well as the construction of the PV power plant and the operation of the PV power plant, are part of the foreground system. The foreground processes are shown with borders and without shading in Figure 1, whereas the background processes are borderless and shaded grey. The processes in the foreground system are established or parametrised in this study, whereas the processes in the background system rely on generic data from various data sources such as the ecoinvent v3.3 database [27,33–36].

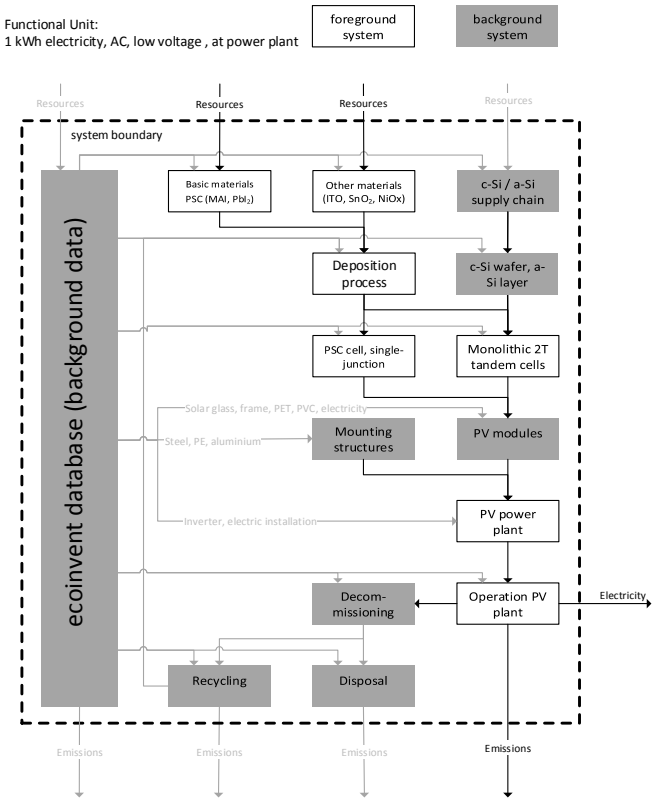

Figure 1. Schematic representation of the perovskite (PSC) and silicon heterojunction (SHJ) production systems, foreground system with border without shading, background system shaded grey; foreground system includes newly established or parametrised processes, whereas the background system relies on generic data from various data sources.

2.3. Life Cycle Impact Assessment

The IEA-PVPS [32] recommends Life Cycle Impact Assessment (LCIA) with a set of 18 different midpoint indicators, including the recommendations by Hauschild et al. [37] in the International Reference Life Cycle Data System (ILCD) Handbook for LCIA and three additional midpoint indicators. This recommended set of LCIA methods was applied in this study and it includes the reporting of greenhouse gas emissions [38], primary energy demand [39] and non-renewable energy payback time (NREPBT). The software SimaPro 8.3 [40] in combination with the ecoinvent database [33] was used for the LCIA.

2.4. Prospective Scenarios and Model Approach

The model approach applied uses process-based LCA data in combination with attributional allocation. The key parameters for wafer based crystalline silicon technologies are subject to prospective future scenarios based on expected future trends. A similar modelling approach was applied in Louwen et al. [4], Frischknecht et al. [29], and Rufer and Braunschweig [30]. These key parameters were modelled based on future projections in the International Technology Roadmap for Photovoltaics (ITRPV) for mono-Si single-junction solar cells [41], in Burschka et al. [42], and in Yang et al. [43] for non-bifacial perovskite single-junction cells and in Werner [10], Albrecht et al. [18], Bush et al. [9], and Almansouri et al. [26] for monolithic 2-two terminal SHJ-PSC tandem cells. The parameters for the different solar cell types are summarised in Table 1. A relative decrease in efficiency of 8.5% from cell to module was assumed for all solar cell types. This corresponds to the current cell to module efficiency ratio for mono-Si solar cells [31]. The ITRPV Roadmap [41] predicts an increase in the cell-to-module power ratio of more than 100% by 2025. However, the realisation of such a high cell-to-module power ratio requires the redirection of sunlight from the inactive module area to the active cell surface and is not included in the prospective scenarios. Global market shares for crystalline silicon production are based on the IEA PVPS LCI report for photovoltaics [31]. These market shares are based on data for the year 2011 and their update was not within the scope of this study. However, the most recent publication of the IEA PVPS Task 1 [44] suggests similar market shares with a high fraction of production in China for 2014. The electricity used for the deposition processes of the additional layers required for the PSC and SHJ cells were modelled with the European electricity mix based on the European Network of Transmission System Operators (ENTSO-E) as implemented in ecoinvent v3.3 [33]. The global market shares for crystalline silicon production as well as the technology composition of the European electricity mix were not subject to changes in the different scenarios.

Table 1. Summary of different prospective scenarios with abbreviation, technology, parameters for cell and module efficiency, wafer thickness, kerf loss, and description including references for parameter values [3,8–10,18,26,31,41–43].

Abbrevia-Tion	Technology	Efficiency in %		Thickness in Micrometer		Description
		Cell	Module	Wafer	Kerf	
Mono-Si REF	Mono-crystalline silicon, single-junction	16.5	15.1	295	145	Reference scenario for the current market average according to IEA PVPS [31]
Mono-Si ITRPV	Mono-crystalline silicon, single-junction	26.0	23.8	140	60	Future scenario according to the ITRPV [41]
Poly-Si REF	Poly-crystalline silicon, single-junction	16.0	14.7	295	145	Reference scenario for the current market average according to IEA PVPS [31]
Poly-Si ITRPV	Poly-crystalline silicon, single-junction	20	18.3	150	60	Future scenario according to the ITRPV [41]
PSC PESS	Perovskite single-junction	15.0	13.8	n.a.	n.a.	Pessimistic scenario with low efficiency for pervovskite single-junction cell [42]

Table 1. *Cont.*

Abbrevia-Tion	Technology	Efficiency in %		Thickness in Micrometer		Description
		Cell	Module	Wafer	Kerf	
PSC OPT	Perovskite single-junction	20.0	18.3	n.a.	n.a.	Optimistic scenario with high efficiency for perovskite single-junction cell [8,26,43]
SHJ-PSC PESS	Monolithic two terminal tandem cell using perovskite and silicon heterojunction tandem	26.0	23.8	295	145	Pessimistic scenario with low efficiency for monolithic two terminal tandem cell using perovskite and silicon heterojunction tandem cell [9,10,18]
SHJ-PSC OPT	Monolithic two terminal tandem cell using perovskite and silicon heterojunction tandem	30.0	27.5	120	60	Optimistic scenario with low efficiency for monolithic two terminal tandem cell using perovskite and silicon heterojunction tandem cell [3,26]

3. Life Cycle Inventory

Life Cycle Inventories (LCI) of two new cell types were established for this study; one of an organometallic halide single-junction perovskite solar cell and one of a monolithic two-terminal tandem cell using an organometallic halide perovskite layer in combination with a silicon heterojunction solar cell. Furthermore, LCIs of different deposition processes were established. These deposition processes were the sputtering of indium tin oxide (ITO), tin oxide (SnO_2), and nickel oxide (NiO_x), as well as the physical vapour deposition of lead iodide (PbI_2) using thermal evaporation and the slot die coating of methyl ammonium iodide (MAI, CH_3NH_3I).

The LCI of the deposition of the amorphous silicon layers for the monolithic SHJ-PSC tandem cell are based on Louwen et al. [4]. The LCI data of cell and module production are based on the LCI data for mono-Si cells and modules (panels) available in the IEA PVPS LCI report [31]. The LCI of cell production includes chemicals for cleaning, screen printing, and metallisation paste for the front and back contacts, including emissions caused by the cleaning agents and the screen printing of the front and back electrodes. The LCI for the panel production includes the interconnection of the cells and encapsulation with ethylene-vinyl acetate (EVA) foil, as well as the aluminium frame and the glass cover for the framed panel.

3.1. Single-Junction PSC

The cell structure of the organometallic halide PSC solar cell is based on the prospective design, which can be produced on an industrial scale with the appropriate deposition processes for industrial production based on published literature [9–12]. This cell structure intentionally excludes deposition processes like spin coating that are not viable for industrial scale production due to the low throughput and high energy demand [34]. Table 2 shows the cell structure for the organometallic halide PSC solar cell used for the LCI. The substrate for the organometallic halide PSC cell is a glass plate with a thickness of 0.7 mm. The PSC cell does not have a front grid but is segmented using laser scribing [45]. The rear contact is made of sputtered silver and the perovskite crystal structure is synthesised based on thermally evaporated lead iodide and slot die coated methyl ammonium iodide, resulting in a methyl ammonium lead iodide layer with a thickness of 500 nm. For the top contact, electron transport, and hole transport, sputtered layers of indium tin oxide, tin oxide, and nickel oxide were used with a thickness of 120 nm, 10 nm, and 10 nm, respectively.

Table 2. Cell structure, including layer thickness, application process, and function of the different layers of the non-bifacial single-junction perovskite cell (PSC) based on organometallic halides [9–12,45].

Layer	Doping	Thickness	Application	Function
Indium tin oxide		120 nm	Sputtering	Top contact layer
Tin oxide	n	10 nm	Sputtering	Electron transport layer
Methyl ammonium lead iodide	i	500 nm	Thermal evaporation of PbI_2 followed by slot-die coating of MAI	Absorber layer
Nickel oxide	p	10 nm	Sputtering or atomic layer deposition	Hole transport material
Silver rear contact		150 nm	Sputtering	Back contact layer

The LCI data on physical vapour deposition processes of PbI_2, ITO, NiO_x, and SnO_2 are derived from ecoinvent v3.3 [33], Classen et al. [35], and Hischier et al. [36]. The solution based deposition of MAI using slot die coating is based on Espinosa et al. [46] and Baldassari et al. [34]. For the sputtering processes, a utilisation rate of 15% was assumed according to Classen et al. [35] and Hischier et al. [36] and implemented in ecoinvent v3.3 [33]. For thermal evaporation and slot die coating, utilisation rates of 50% and 80% were assumed according to the suggested utilisation rates for vacuum deposition in Classen et al. [35] and the technical data sheets of slot die coating devices [47]. The MAI is dissolved in isopropanol for the slot die coating process with a concentration of 6 wt % according to Werner et al. [10] and Espinosa et al. [46], which corresponds to 41 g of isopropanol per square meter of deposited area with a utilisation rate of 20%. The isopropanol solvent used was modelled as direct emissions to air. The LCI data for the PbI_2 and MAI are based on Gong et al. [14]. The LCIs of the deposition processes and raw materials are shown in detail in the supporting information.

3.2. Monolithic 2-Terminal SHJ-PSC Tandem

The cell structure of the non-bifacial monolithic 2-terminal tandem cell using an organometallic halide perovskite layer and silicon heterojunction solar cell shown in Table 3 is based on published literature [3,9–12] as shown in Table 1. The major differences in the cell are the addition of the mono-Si silicon wafer as a substrate and the amorphous silicon layers for the silicon heterojunction cell, as well as an additional ITO layer between the back surface field and the back contact required for the sputtering of the rear contacts on the amorphous silicon layers. The mono-Si wafer was modelled with a thickness of 295 and 120 mm. The deposition processes for the organometallic halide perovskite layer are identical to the deposition processes used for the PSC single-junction cell. The amorphous silicon layers are deposited by plasma enhanced chemical vapour deposition (PECVD) and were modelled based on the LCI data of Louwen et al. [4]. The same utilisation rates for the other deposition processes were used as were used for the organometallic halide PSC single-junction for the monolithic SHJ-PSC tandem. The SHJ-PSC tandem cell has a front and back grid made of screen printed and sputtered silver, respectively.

Table 3. Cell structure including layer thickness, application process, and function of the different layers of the non-bifacial monolithic 2-terminal tandem cell using an organometallic halide perovskite layer and a silicon heterojunction solar cell [3,9–12].

Layer	Doping	Thickness	Application	Function
Ag front grid			Ag screen printing	Front grid
Indium tin oxide		80 nm	Sputtering	Top contact layer
Nickel oxide	p	10 nm	Sputtering or atomic layer deposition	Hole transport
Perovskite	i	500 nm	Thermal evaporation of PbI_2 followed by slot-die coating of MAI	Absorber layer
Tin oxide	n	10 nm	Sputtering	Electron transport
n-μ-c-Si	n	10 nm	PECVD	Recombination junction
p-μ-c-Si	p	10 nm	PECVD	Recombination junction
i-a-Si	i	10 nm	PECVD	Passivation
n-Si	n	295 and 120 micron	Base for others layers	Silicon substrate
i-a-Si	i	10 nm	PECVD	Passivation
n-a-Si	n	10 nm	PECVD	Back surface field
Indium tin oxide		100 nm	Sputtering	Back contact layer
Ag rear contact		200 nm	Sputtering	Back electrode

3.3. Long-Term Stability

The industrialisation of perovskite solar cells requires the stability of the synthetic perovskite crystal structure and conversion efficiency [8]. Berhe et al. [7] highlight multiple causes of the degradation of perovskite solar cells including oxygen, light, moisture, and thermally induced degradation. However, Saliba et al. [8] and Beal et al. [13] showed that the addition of caesium to the synthetic perovskite crystal structure can increase thermal stability as well as stability under full illumination, resulting in a degradation to only 85% of the original efficiency after prolonged illumination of 250 h. Furthermore, You et al. [12] report improved stability for water and oxygen induced degradation if the PSC layer is combined with inorganic materials as hole and electron transport layers instead of organic materials. Zhu et al. [11] report the stability of the synthesised PSC under a controlled and humid atmosphere of up to one month if the PSC layer is combined with nickel and tin oxide. Additionally, Bush et al. [9] report improved stability of monolithic silicon-PSC tandem cells that were resistant to 1000 h damp heat tests at high temperatures and humidity. According to Berhe et al. [7] the recent improvements regarding PSC cell stability are promising for a successful practical application. The cell structures as described in Tables 2 and 3 use SnO_2 and NiO_x as the inorganic hole and electron transport layer for improved stability. The PSC solar cells are combined in tandem cells with crystalline silicon cells, which have a proven lifetime of 30 years of more. Therefore, an optimistic lifetime of 30 years with a linear degradation rate of 0.7% per year was used for PSC solar cells, which corresponds to the recommended lifetime and degradation according to the IEA PVPS methodology guideline [32] for crystalline silicon solar cells. Due to the uncertainty about the lifetime and degradation of PSC solar cells, different lifetimes and degradation rates were analysed in a sensitivity analysis.

3.4. Other Data Sources

The LCI data on the crystalline silicon supply chain, cell and module production as well as market information for the silicon supply chain are based on the IEA-PVPS LCI report [31], and data on the mounting system, inverter, and operation are based on Jungbluth et al. [48] and ecoinvent [33]. A framed module is used for the encapsulation of all cell types. For crystalline silicon based cells encapsulation in an unframed laminate is possible, reducing material demand. However, considering the necessity of a fail-safe encapsulation for PSC, the unframed laminate was not considered an alternative. The data on the photovoltaic yield in central Europe (Austria) were based on the annual photovoltaic electricity output of 1027 kWh per kWp according to EPIA [49]. This corresponds to an annual yield of 919 kWh per kWp, including 0.7% linear degradation per year (10.5% on average for a lifetime of 30 years) and a total lifetime electricity yield of 27,570 kWh for a lifetime of 30 years.

4. Results and Discussion

4.1. Prospective Life Cycle Environmental Impacts

The comparison of the current and prospective environmental impacts of photovoltaic electricity produced by the different solar cell types including future scenarios for the most crucial parameters, shown in Figure 2 reveals that SHJ-PSC-PESS and SHJ-PSC-OPT cause lower environmental impacts than mono-Si-REF and mono-Si-ITRPV for all midpoint indicators except for mineral and fossil resource use. The resource use impacts for mono-Si-REF and mono-Si-ITRPV (and poly-Si REF and poly-Si ITRPV) are significantly lower than SHJ-PSC-PESS and SHJ-PSC-OPT (PSC-PESS and PSC-OPT, <20%); this a clear trade-off between mineral and fossil resource use and the other midpoints. The use of ITO as a transparent conductive oxide (TCO) in the PSC and SHJ cell structure causes high resource use due to the utilisation of indium. Candelise et al. [50] report the use of scarce indium as a potential barrier for thin film photovoltaics like CIGS due to indium supply constraints. Arvidsson et al. [51] highlight the environmental impacts of the use of indium as a scarce resource in liquid crystal displays, which are used in electronic devices like phones, tablets, computers, and televisions. Nevertheless, indium is

the most interesting resource for urban mining according to Zimmermann et al. [52] due to its wide use in a variety of electronic devices combined with its high price, scarcity, and low supply. The use of PSC single-junction cells and, to a lesser extent, PSC-SHJ tandems, can reduce the environmental impacts for all midpoints except mineral and fossil resource depletion, provided that the lifetime of the PSC cells is increased to an optimistic 30 years. This reduction of environmental impacts is mainly caused by the lower energy demand required for the deposition of the PSC layer compared to the production of crystalline silicon wafers. The direct comparison of crystalline silicon and SHJ cells is not shown in Figure 2. However, Louwen et al. [4] provide detailed results for this comparison.

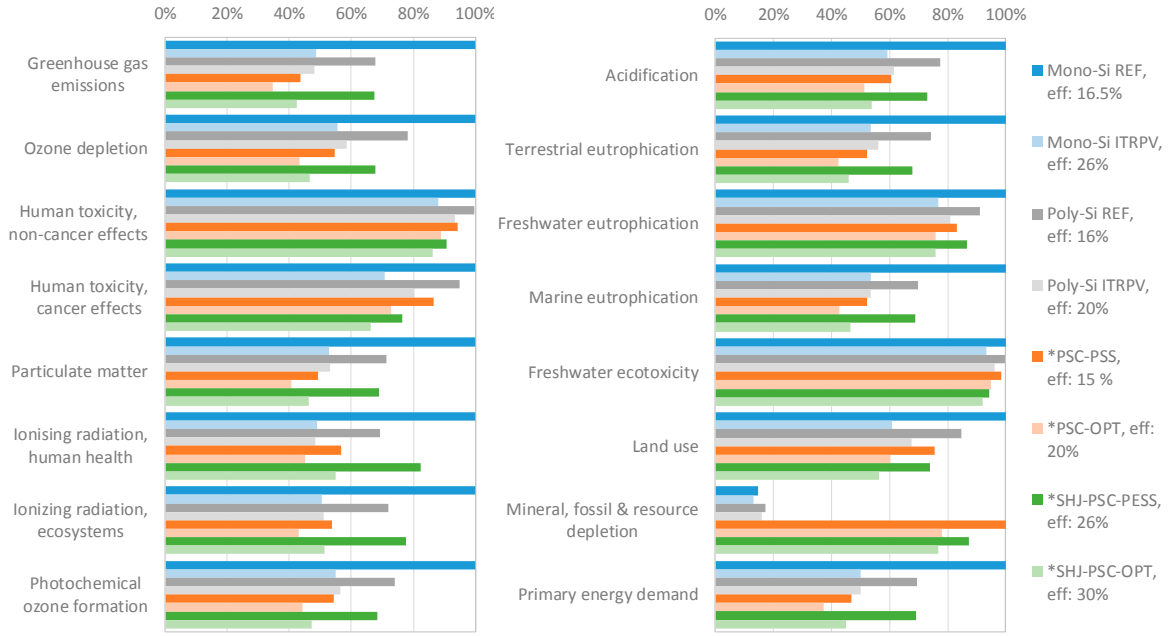

Figure 2. Comparison of life cycle based impacts caused by different PV power plants for greenhouse gas emission, ozone depletion, human toxicity non-cancer, human toxicity cancer, particulate matter, ionising radiation, photochemical ozone formation, acidification, terrestrial eutrophication, freshwater eutrophication, marine eutrophication, freshwater ecotoxicity, land use, mineral and fossil resource depletion, and primary energy demand [32,37] per kWh of low voltage electricity produced at inverter; with installation on a roof-top in Central Europe with actual electricity yield 919 kWh per kWp and year including average degradation of 10.5% with a lifetime of 30 years; * optimistic lifetime of 30 years for the perovskite solar cell (PSC) layer.

4.2. Comparison Literature: Electricity Demand and Greenhouse Gas Emissions

The electricity demand for the production of photovoltaic cells not only depends on the wafer type and deposition process but also on the scale of production. Figure 3 shows the electricity demand for the different processing steps in the photovoltaic supply chain for different cell technologies, production scales, and deposition processes. This figure reveals high variability in electricity demand in the different published results for PSC depending on the scale of production. Baldassarri et al. [34] highlight the differences in electricity demand between spin coating and other deposition techniques like sputtering and slot die coating. Laboratory spin coating is ranked as having the highest energy demand with the lowest throughput [34]. The electricity demand for the production of one square meter mono-crystalline silicon wafer including the crystalline silicon supply chain is 290 kWh for mono-Si REF and 140 kWh for mono-Si ITRPV compared to the demands of deposition of the PSC and SHJ layers on an industrial scale of 14 and 24 kWh, respectively.

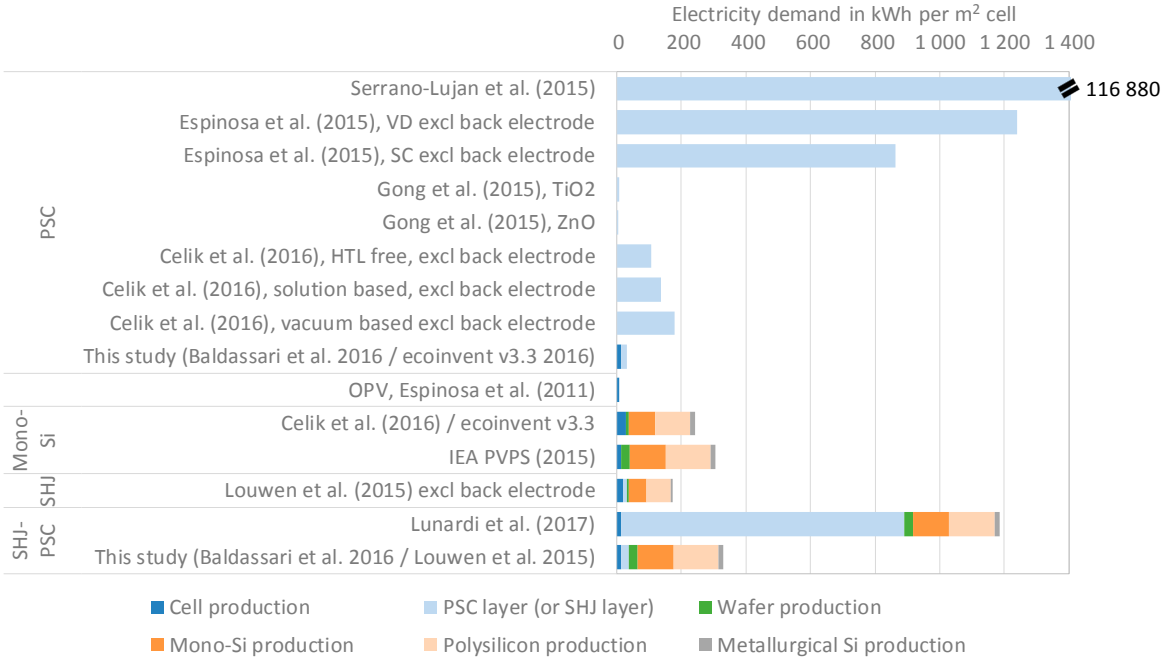

Figure 3. Comparison of the electricity demand for the different processing steps in the photovoltaic supply chain for different cell technologies, production scales, and cell structures according to Serrano-Lujan et al. [16], Espinosa et al. [15], Gong et al. [14], Celik et al. [17], ecoinvent v3.3 [33], Baldassarri et al. [34], Espinosa et al. [46], IEA-PVPS [31], Louwen et al. [4], and Lunardi et al. [28].

The electricity used for the deposition processes of the additional layers required for the PSC and SHJ cells was modelled with the European electricity mix based on the European Network of Transmission System Operators (ENTSO-E) as implemented in ecoinvent v3.3 [32]. The differences in the electricity demand for cell production cause similar differences in the life cycle environmental impacts of energy related LCIA methods like greenhouse gas emissions. Celik et al. [17] harmonised the greenhouse gas emissions per kWh of electricity produced by PSC solar cells published in the recent literature for a lifetime of fivr years but did not include the life cycle greenhouse gas emissions caused by the mounting system, the module, and cell production, as well as the required inverters. Figure 4 shows the harmonised comparison in [17] for a lifetime of 30 years including the life cycle greenhouse gas emissions of the inverter, mounting system, cell, and module production. The different electricity demand as shown in Figure 3 directly influences the result for greenhouse gas emissions. The deposition of the PSC layer causes a large share of the total life cycle of greenhouse gas emissions for lab scale production. However, in the case of scaled industrial production, the contribution of the PSC layer is only minor.

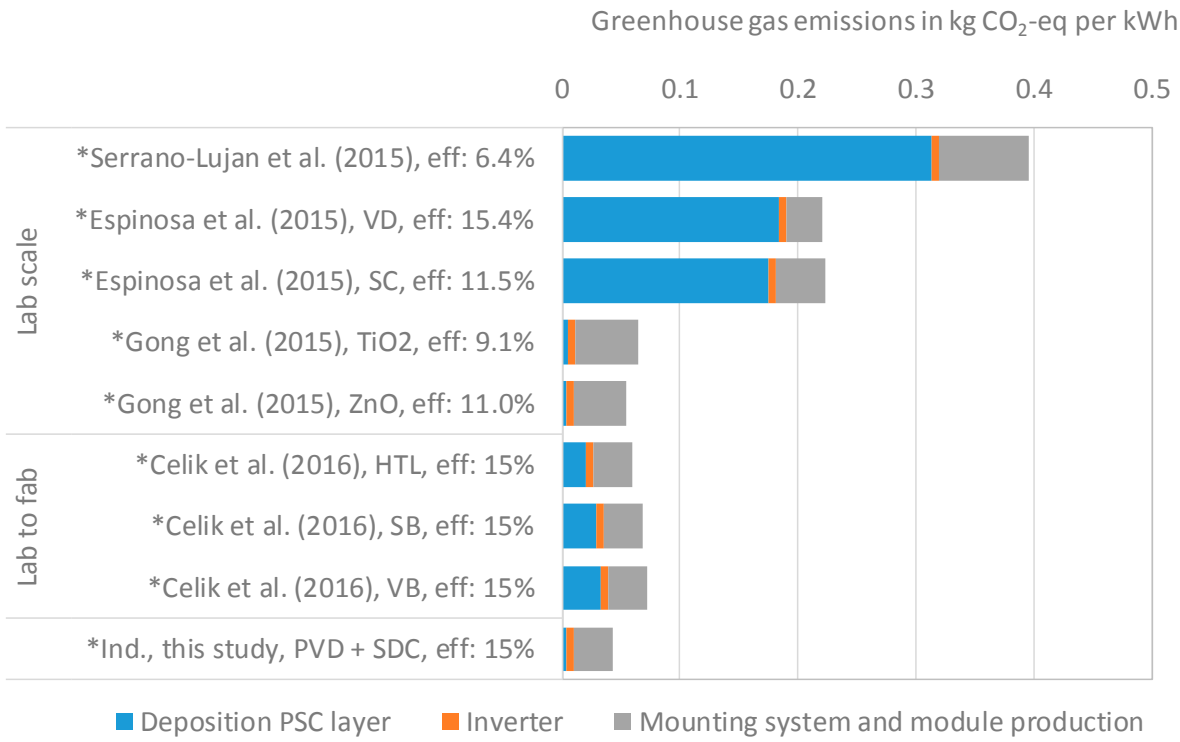

Figure 4. Comparison of harmonised greenhouse gas emissions per kWh of low voltage electricity produced by perovskite solar cells (PSC) according to Serrano-Lujan et al. [16], Espinosa et al. [15], Gong et al. [14], and Celik et al. [17], including the contribution of inverter, mounting system, module, and cell production; harmonised yield and lifetime with standard insolation of 1700 kWh/m^2·y and a performance ratio of 0.75%; electricity yield of 1275 kWh per kWp and year, excluding degradation with a lifetime of 30 years; * optimistic lifetime of 30 years for PSC layer.

4.3. Potential Toxicity Induced by PSC Layer Composition

Another important environmental impact to consider is toxicity due to heavy metals such as lead and tin that are contained in the synthetic perovskite crystal structure. However, Hailegnaw et al. [53] determined no catastrophic toxicity impacts even for the total destruction of the solar power plant and the direct exposure of the cell to rain. The full leakage of the lead contained in the PSC layer (less than one gram per square meter) will only cause an increase in lead concentrations in the ground below to around 70 ppm. According to Hailegnaw et al. [53], these concentrations 'cannot be considered even close to disastrous' compared to the concentration of 30 ppm in natural uncontaminated soil and 50 to 200 ppm in urban areas. Babayigit et al. [54] analysed the toxicity impacts of the heavy metal containing compounds PbI_2 and SnI_2 on zebrafish. They revealed that the heavy metal salts PbI_2 and SnI_2 decompose to very strong hydroiodic acid, causing higher lethality for the zebrafish due to acidification than due to the presence of heavy metals. Furthermore, Babayigit et al. [55] highlight the importance of correct handling and the importance of the fail-safe encapsulation of the perovskite solar cells, which is not only required for the safe use for the PSC solar cells but is also required to improve the stability of the PSC cell. If the PSC cells are embedded in proper encapsulation as well as handled and disposed of correctly, the toxicity impacts of the heavy metals used in PSC cells are considered to be minimal.

4.4. Contribution Analysis for Greenhouse Gas Emissions

The carbon footprint, including the contribution of the different parts of the photovoltaic power plant shown in Figure 5, corresponds to 56 g CO_2-eq per kWh for the scenario mono-Si REF. In this case,

the mono-Si wafer (43%), the photovoltaic module production (18%), the mounting system (16%), and the electric inverter (11%) are the main contributors. For PSC-OPT, the carbon footprint is 40 g CO_2-eq per kWh, with the module production (36%), the mounting system (30%), the electric inverter (16%), and the PSC cell (7%) as the main contributors. For SHJ-PSC-OPT, the carbon footprint is 47 g CO_2-eq per kWh, with the mono-Si wafer (37%), photovoltaic module production (16%), mounting system (16%), electric inverter (13%), and the SHJ-PSC layer (6%) as the main contributors (see Figure 5). These results are valid for slanted-roof installations in central Europe with an actual electricity yield of 919 kWh per kW_p, including an average degradation of 10.5% (0.7% per year) with a lifetime of 30 years.

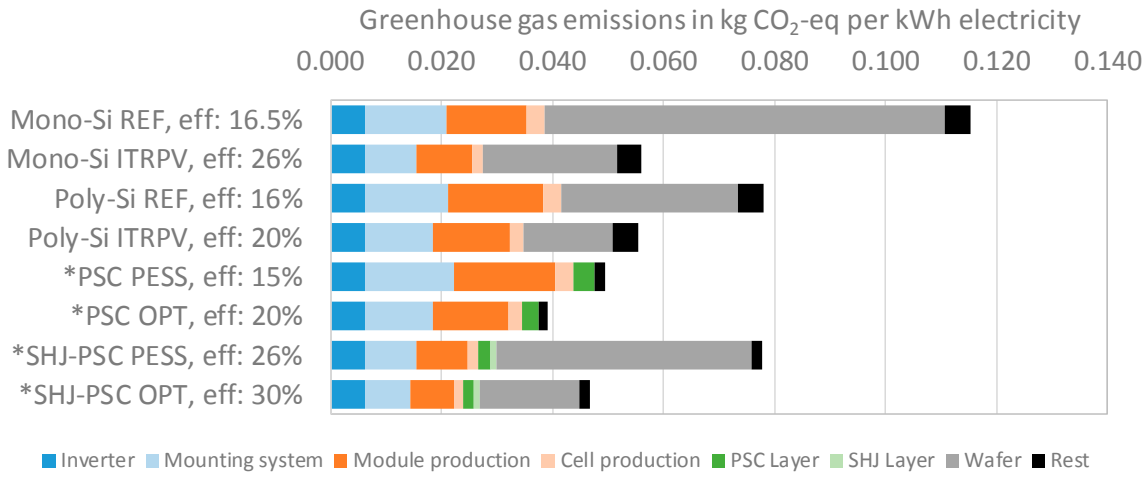

Figure 5. Contribution of the different components of the photovoltaic power plant to the life cycle greenhouse gas emissions per kWh of low voltage electricity produced at the inverter; with installation on a rooftop in central Europe with an actual electricity yield of 919 kWh per kWp and year, including an average degradation of 10.5% with a lifetime of 30 years; * optimistic lifetime of 30 years for PSC layer.

The single-junction PSC is the photovoltaic technology with the lowest carbon footprint per kWh of electricity produced given that the lifetime of the PSC solar cell is 30 years and the annual degradation is not more than 0.7% per year (10.5% on average for a lifetime of 30 years). The low energy demand for the production of the PSC layer compared to the production of the silicon wafer in combination with the comparable efficiency of PSC solar cells ranging between 16 to 20% reduces the carbon footprint of the PSC solar cells to below that of crystalline silicon based solar cells. The production of the PSC layer causes only between 5 and 12% of the greenhouse gas emissions of the mono-Si wafer (and between 11 and 18% of the poly-Si wafer). The 30-year lifetime with degradation of 0.7% per year used for the underlying calculations of the results shown in Figure 5 is very optimistic for single-junction PSC compared to the current lifetime [6–13]. However, per kWh of electricity produced, a relevant share of the life cycle greenhouse gas emissions is caused by the production of the module and the balance-of-system components like the inverter and the mounting system. For the life cycle greenhouse gas emissions of the PSC to be lower than the crystalline silicon cells, the PSC solar cells have to achieve a similar lifetime. Otherwise, the life cycle greenhouse gas emissions per kWh of electricity produced by PSC solar cells will be higher than crystalline silicon based solar cells, mainly due to the high greenhouse gas emissions caused by the production of the mounting systems, modules, cells, and inverters.

The additional layers required for the SHJ and PSC cells are comparable due to the similarity of the deposition techniques used (thermal evaporation and sputtering) and the layer thickness. However,

the deposition of the additional SHJ layers causes lower greenhouse gas emissions than the deposition of the PSC layer.

4.5. Sensitivity Analysis for Lifetime and Degradation

Due to the currently limited stability and lifetime of the PSC solar cell, a comparison of the mono-Si cells with a lifetime of more than 30 years is not fully appropriate. In order to enable a fair comparison of different cell types, we calculated the life cycle greenhouse gas emissions of the PSC solar cells with variable lifetimes from one to 30 years relative to the life cycle greenhouse gas emissions of mono-Si solar cells with a fixed lifetime of 30 years as recommended by the IEA-PVPS methodology guideline [32]. Figure 6 shows the result range calculated for the scenarios mono-Si-REF, mono-Si-ITRPV, poly-Si-REF, and poly-Si ITRPV, as well as the intersection with the lifetime dependent scenarios for PSC-PESS and PSC-OPT (or SHJ-PSC-PESS and SHJ-PSC-PESS). The life cycle greenhouse gas emissions per kWh of electricity produced by PSC-PESS are lower compared to mono-Si REF if the lifetime of the PSC cell exceeds 12 years. However, if the benchmark for the PSC cells is the prospective scenario for mono-crystalline silicon-based solar cells mono-Si ITRPV, the benchmarks for the lifetimes increases to 27 and 21 years for the scenarios PSC-PESS and PSC-OPT, respectively.

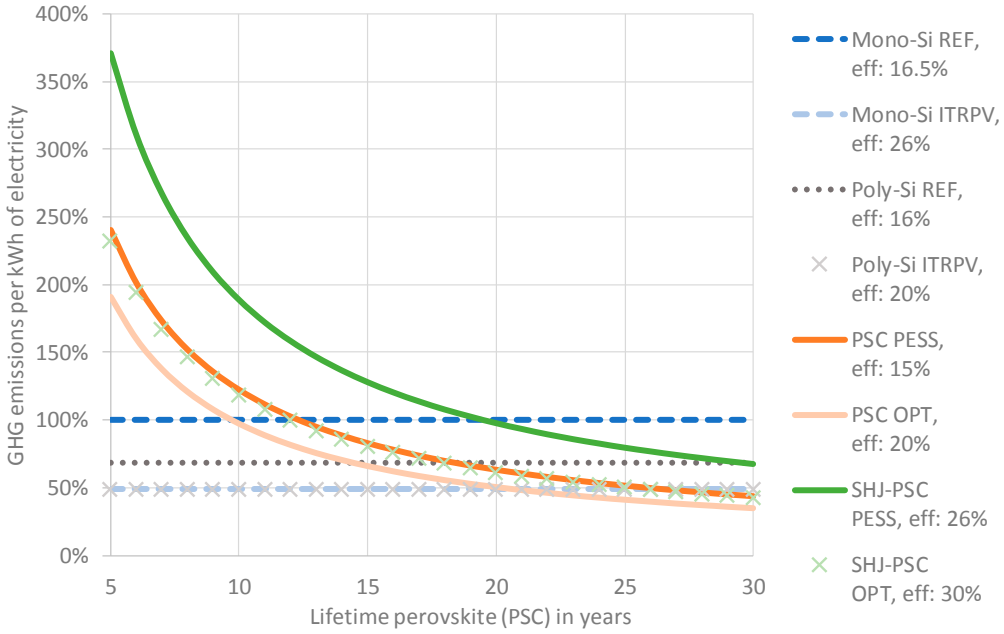

Figure 6. Life cycle greenhouse gas emissions per kWh of low voltage level electricity produced at inverter depending on the lifetime relative to mono-Si-REF silicon with a given lifetime of 30 years; installation on a rooftop in central Europe with actual electricity yield 919 kWh per kWp and year including an average degradation of 0.7% per year; lifetime variable for PSC and SHJ-PSC tandem.

The comparison of the single-junction PSC and the SHJ-PSC tandem reveals that the SHJ-PSC tandem will not outperform the single-junction PSC in terms of life cycle greenhouse gas emissions per kWh of electricity produced with the given efficiency increase according to the prospective scenarios summarised in Table 1. The module efficiency of the SHJ-PSC tandem cell is 9.2% higher than the PSC single junction cells. However, due to the negligible environmental impact of the PSC layer compared to the mono-Si wafer, the increase in efficiency of 9.2% is not sufficient to reduce the life cycle greenhouse gas emissions per kWh of electricity produced by SHJ-PSC tandem cells below those of electricity produced by PSC single-junction cells. However, the life cycle greenhouse gas emissions of SHJ-PSC-OPT are lower compared to the prospective scenarios Mono-Si-REF and Poly-Si-REF if the lifetime of the PSC layer exceeds 27 years. Single-junction PSC solar cells and SHJ-PSC tandem cells

will be able to outperform future first generation mono-Si solar cells if the lifetime of the PSC is at least 21 years and 27 years, respectively.

The lifetime is not the only important variable in the case of PSC solar cells. According to Berhe et al. [7], the PSC also degrade faster when exposed to oxygen, light, moisture, or high temperatures compared to silicon based solar cells. In order to account for this increased degradability, we increased the degradation rate for the PSC single-junction cell from 0.7% linear degradation per year, which corresponds to 10.5% per year on average for a lifetime of 30 years, to 1.5%, 3%, 5%, and 10%.

For a degradation rate of 10% and 5% per year, the lifetime of the PSC cell is only 10 and 20 years since electricity production will be zero after year 10 and 20, respectively. Figure 7 shows the comparison of the PSC-OPT, subject to different degradation rates with Mono-Si REF, Poly-Si REF, Mono-Si ITRPV, and Poly-Si ITRPV. The end of life (EoL) of the perovskite cells with high degradation is marked with EoL. Figure 7 shows that an increase in the degradation rate from 0.7% to 3% for perovskite cells with optimistic efficiency (PSC-OPT) results in higher greenhouse gas emissions per kWh of electricity produced compared to the mono-Si ITRPV and Poly-Si ITRPV scenarios, even if a lifetime of 30 years can be achieved for the PSC solar cells. Accordingly, a PSC single-junction cell with 20% efficiency has to exceed a lifetime of 24 years with less than 3% degradation per year in order to be competitive with the crystalline silicon single-junction cells.

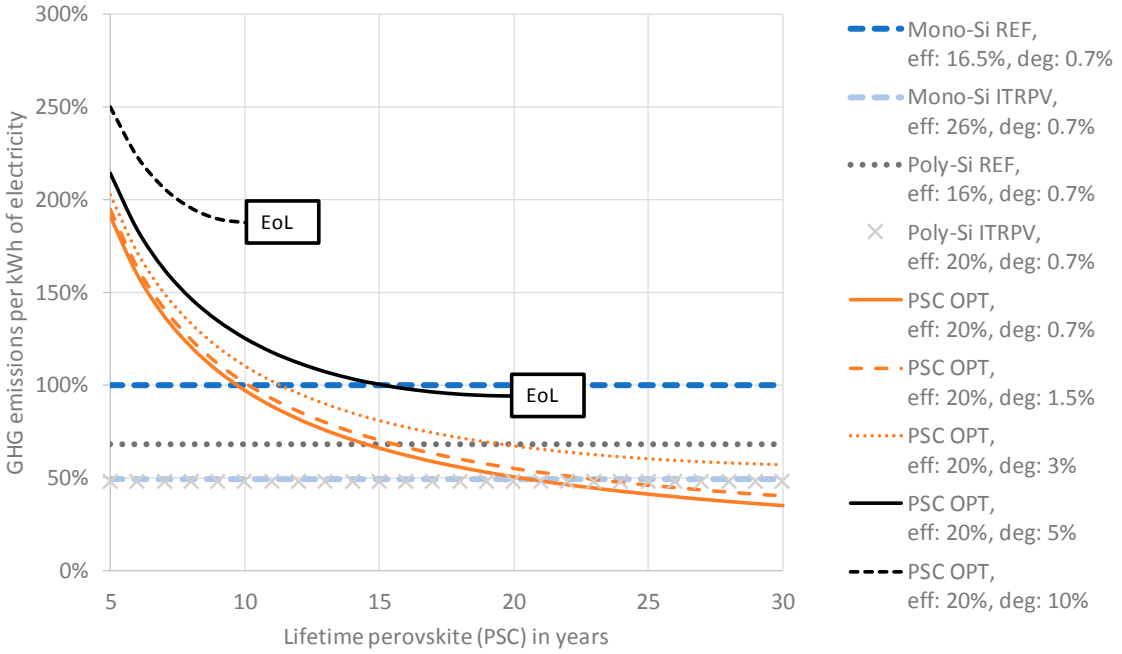

Figure 7. Life cycle greenhouse gas emissions per kWh of low voltage electricity produced at inverter; depending on the lifetime and degradation relative to mono-Si-REF (with a given lifetime of 30 years and annual degradation of 0.7%); installation on a rooftop in central Europe with actual electricity yield 919 kWh per kWp and year; lifetime variable for PSC; degradation rates of 0.7%, 1.5%, 3%, 5%, and 10% for PSC cells.

4.6. Surface Area Demand and Non-Renewable Energy Payback Time (NREPBT)

In most European countries, there is only limited space available for photovoltaic installations [56]. PV technologies with higher module efficiency reduce the required surface area and thus allow for a higher installation of PV capacity on a national level. Figure 8 shows how the area required per kWp of photovoltaic power plant is reduced with increasing efficiency. With this decreased area demand for electricity production, the material demand for mounting systems is also reduced. The

area requirements of the tandem cells are significantly lower compared to the other cell types due to the increased efficiency of the tandem cells. Compared to a PSC single junction cell with an efficiency of 15% a PSC-SHJ tandem cell with 30% efficiency only requires 50% of the area for the same peak power. If the installed PV capacity has to be maximised with only limited surface area available, the SHJ-PSC tandem would be preferred over the PSC single-junction because their environmental impacts are similar, but the surface area demand of SHJ-PSC tandems is only 70% or less of the PSC single-junction cells.

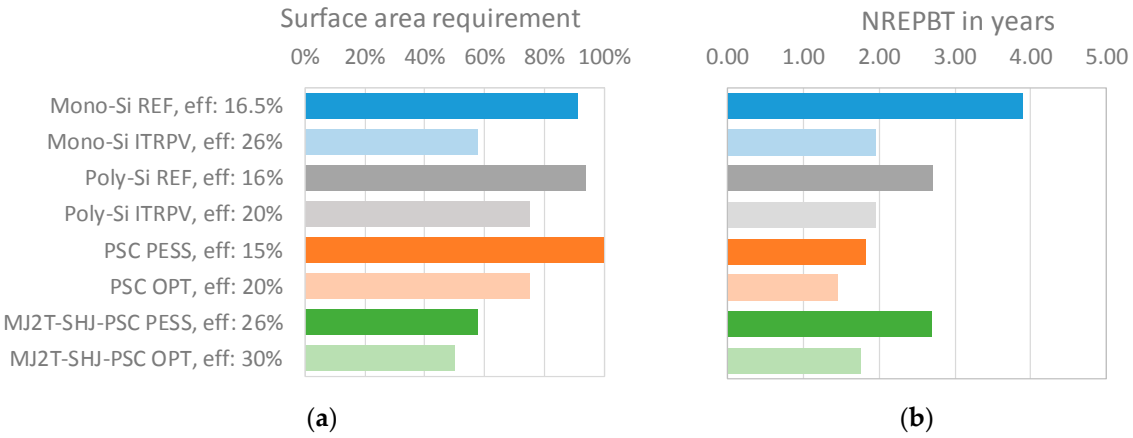

Figure 8. (**a**) Surface area requirements per kWp relative to the surface area requirement of PSC cells with a cell efficiency of 15% (**b**) and non-renewable energy payback time (NREPBT) in years for installation in central Europe; actual yield 919 kWh per kWp and year including 10.5% degradation; grid efficiency for Central Europe: 0.36, based on ENTSO-E electricity mix [32,33].

The non-renewable energy payback time (NREPBT) according to the IEA PVPS methodology guideline on LCA of photovoltaic electricity [32] is calculated as the ratio of the non-renewable primary energy demand of the complete photovoltaic power plant including balance-of-system components in MJ oil-eq and the annual mitigated primary energy demand caused by the produced photovoltaic electricity in MJ oil-eq per year according to Frischknecht et al. [39]. The comparison of the NREPBT of the different photovoltaic cell types in Figure 8 reveals that the mono-Si-REF has the highest NREPBT with 3.9 years, followed by the SHJ-PSC PESS and mono-Si-ITRPV with 2.7 and 2.0 years, respectively. The PSC-OPT has the lowest NREPBT with 1.5 years, followed by SHJ-PSC-OPT and PSC-PESS with 1.7 and 1.8 years, respectively. The NREPBT calculations are valid for central Europe with an actual yield of 919 kWh/kWp, including 10.5% degradation and a grid efficiency of 0.36, which corresponds to a primary energy demand of 9.87 MJ oil-eq per kWh of electricity according to the European ENTSO-E grid mix on the low voltage level in ecoinvent v3.3 [33]. The low NREPBT of PSC cells is caused by the low electricity demand for the production of the PSC layer compared to the crystalline silicon wafers.

4.7. Limitations, Data Quality Considerations and Future Research Requirements

The scope of the study is appropriate for the comparison of crystalline silicon, PSC and SHJ-SPC tandem solar cells. However, there are some limitations. The prospective scenarios in this paper do not include scenarios for future electricity mixes, future market shares in the crystalline silicon supply chain, future cell and module production, and future mounting systems for building integration. The electricity mix as an important factor for the environmental impacts, especially for the crystalline silicon solar cells, was not subject to prospective scenarios. Significant changes in the technology composition of the electricity mixes, especially in China, the US, and Europe have to be expected by the year 2025. However, changes in the underlying electricity mix will affect the results of all cell types and therefore are not crucial for the comparisons in this paper. We used the same LCI data for the

encapsulation in modules for all cell technologies; mainly due to a lack of specific information about the encapsulation of PSC single junction and SHJ-PSC tandem cells. Furthermore, we did use not prospective scenarios for mounting systems and inverters. The unchanged LCI for module production, inverters, and mounting systems leads to a relevant increase in contribution of these balance-of-system components in the final results, especially for solar cells with low environmental impacts like PSC solar cells.

The data quality in general is considered high. The LCI data for the crystalline supply chain and the SHJ solar cells are based on recent results [4,31] as well as the PSC cell structure [9–12,25]. The deposition processes for the PSC layer are based on older data [35,36,46] due to the lack of primary industrial data. We used conservative utilisation rates of these deposition processes in order to account for the low data quality. However, even with these conservative utilisation rates, the deposition process of the PSC (and SHJ) layers does not have a major contribution to the final results.

Future research is still required to reduce the degradation under real operating conditions and increase the stability of the PSC layer. Also, the failsafe encapsulation and the efficient integration of the photovoltaic modules into buildings become more relevant with the continuous improvement of solar cells. Encapsulation directly influences the stability and the toxicity impacts as well indirectly influences other environmental impacts via the materials used for the encapsulation. In the case of the PSC solar cell, less material intensive encapsulation, which still meets the high requirements for PSC solar cells, could reduce the total environmental impacts significantly. The same applies to more efficient mounting systems that have reduced material demand. Both these aspects can be tackled with a direct integration of the photovoltaic power plant into the building, reducing the demand for additional mounting systems.

5. Conclusions

This study compared the environmental impacts of monolithic tandem cells using silicon heterojunction and organometallic perovskite solar cells (SHJ-PSC) and single junction organometallic perovskite solar cells (PSC) with the impacts of crystalline silicon based solar cells using a prospective life cycle assessment with time horizon of 2025. The analysis showed that, the stability of the PSC layer is not only crucial for economic and industrial viability, but is also the most important factor for environmental impacts. The toxicity and resource use impacts of the PSC layer are tied to the materials used. Therefore, adjustments in the structure of the PSC layer have to be re-evaluated regarding toxicity and mineral resource use. The electricity demand for the deposition of the PSC layer and crystalline silicon wafer production is crucial for most environmental impacts including greenhouse gas emissions and NREPBT. The lifetime of the PSC layer has to exceed at least 20 years in order to be environmentally competitive with crystalline silicon solar cells. However, this requires major improvements in the stability of the PSC cells, which currently only have stabilised efficiency for several hundred hours. Given a comparable lifetime with crystalline silicon solar cells, the PSC single junction and, to a lesser extent, SHJ-PSC tandem solar cells cause similar or lower environmental impacts than crystalline silicon solar cells, with the SHJ-PSC tandem solar cell having a considerably lower surface area requirement compared to the limited efficiency PSC single junction solar cell. Accordingly, the SHJ-PSC tandem cells should be preferred to crystalline silicon and PSC single-junction cells if the photovoltaic yield has to be maximised with minimal environmental impacts and only limited surface area available.

Supplementary Materials: Supplementary materials can be found at www.mdpi.com/1996-1073/10/7/841/s1.

Acknowledgments: This work received financial support from the Swiss National Science Foundation via the NRP70 'Energy Turnaround' project 'PV2050: Sustainability, market deployment and interaction with the grid—the impacts of advanced photovoltaic solutions'. The authors would like to thank B. Niesen, the Centre Suisse d'Electronique et de Microtechnique (CSEM), the École Polytechnique Fédérale de Lausanne (EPFL) Photovoltaics and Thin Film Laboratory (PV-Lab), for the input on the perovskite structures, and K. Muir, Zurich University of Applied Sciences Research Group Life Cycle Assessment for the English editing.

Author Contributions: Matthias Stucki and René Itten designed the conceptual approach; René Itten wrote the paper and performed the underlying calculations and literature research. Matthias Stucki provided feedback on the paper and the underlying methodology.

Conflicts of Interest: The founding sponsors had no role in the design of the study; in the collection, analyses, or interpretation of data; in the writing of the manuscript; or in the decision to publish the results.

References

1. Intergovernmental Panel on Climate Change (IPCC). Contribution of Working Group III to the Fifth Assessment Report of the Intergovernmental Panel on Climate Change. In *Climate Change 2014: Mitigation of Climate Change*; Cambridge University Press: Cambridge, UK, 2014.
2. IEA World Energy Balances. *Key World Energy Trends*; International Energy Agency (IEA): Paris, France, 2016.
3. De Wolf, S.; Descoeudres, A.; Holman, Z.C.; Ballif, C. High-efficiency silicon heterojunction solar cells: A review. *Green* **2012**, *2*, 7–24. [CrossRef]
4. Louwen, A.; van Sark, W.G.J.H.M.; Schropp, R.E.I.; Turkenburg, W.C.; Faaij, A.P.C. Life-cycle greenhouse gas emissions and energy payback time of current and prospective silicon heterojunction solar cell designs. *Prog. Photovolt. Res. Appl.* **2015**, *23*, 1406–1428. [CrossRef]
5. Snaith, H.J. Perovskites: The emergence of a new era for low-cost, high-efficiency solar cells. *J. Phys. Chem. Lett.* **2013**, *4*, 3623–3630. [CrossRef]
6. Zhou, H.; Shi, Y.; Dong, Q.; Zhang, H.; Xing, Y.; Wang, K.; Du, Y.; Ma, T. Hole-conductor-free, metal-electrode-free TiO2/CH3NH3PbI3 Heterojunction solar cells based on a low-temperature carbon electrode. *J. Phys. Chem. Lett.* **2014**, *5*, 3241–3246. [CrossRef] [PubMed]
7. Berhe, T.A.; Su, W.-N.; Chen, C.-H.; Pan, C.-J.; Cheng, J.-H.; Chen, H.-M.; Tsai, M.-C.; Chen, L.-Y.; Dubale, A.A.; Hwang, B.-J. Organometal halide perovskite solar cells: Degradation and stability. *Energy Environ. Sci.* **2016**, *9*, 323–356. [CrossRef]
8. Saliba, M.; Matsui, T.; Seo, J.-Y.; Domanski, K.; Correa-Baena, J.-P.; Nazeeruddin, M.K.; Zakeeruddin, S.M.; Tress, W.; Abate, A.; Hagfeldt, A.; et al. Cesium-containing triple cation perovskite solar cells: Improved stability, reproducibility and high efficiency. *Energy Environ. Sci.* **2016**, *9*, 1989–1997. [CrossRef] [PubMed]
9. Bush, K.A.; Palmstrom, A.F.; Yu, Z.J.; Boccard, M.; Cheacharoen, R.; Mailoa, J.P.; McMeekin, D.P.; Hoye, R.L.Z.; Bailie, C.D.; Leijtens, T.; et al. 23.6%-efficient monolithic perovskite/silicon tandem solar cells with improved stability. *Nat. Energy* **2017**, *2*, 17009. [CrossRef]
10. Werner, J.; Barraud, L.; Walter, A.; Bräuninger, M.; Sahli, F.; Sacchetto, D.; Tétreault, N.; Paviet-Salomon, B.; Moon, S.-J.; Allebé, C.; et al. Efficient near-infrared-transparent perovskite solar cells enabling direct comparison of 4-terminal and monolithic perovskite/silicon tandem cells. *ACS Energy Lett.* **2016**, *1*, 474–480. [CrossRef]
11. Zhu, Z.; Bai, Y.; Liu, X.; Chueh, C.-C.; Yang, S.; Jen, A.K.-Y. Enhanced efficiency and stability of inverted perovskite solar cells using highly crystalline SnO_2 Nanocrystals as the robust electron-transporting layer. *Adv. Mater.* **2016**, *28*, 6478–6484. [CrossRef] [PubMed]
12. You, J.; Meng, L.; Song, T.-B.; Guo, T.-F.; Yang, Y.; Chang, W.-H.; Hong, Z.; Chen, H.; Zhou, H.; Chen, Q.; et al. Improved air stability of perovskite solar cells via solution-processed metal oxide transport layers. *Nat. Nanontechnol.* **2016**, *11*, 75–81. [CrossRef] [PubMed]
13. Beal, R.E.; Slotcavage, D.J.; Leijtens, T.; Bowring, A.R.; Belisle, R.A.; Nguyen, W.H.; Burkhard, G.F.; Hoke, E.T.; McGehee, M.D. Cesium lead halide perovskites with improved stability for tandem solar cells. *J. Phys. Chem. Lett.* **2016**, *7*, 746–751. [CrossRef] [PubMed]
14. Gong, J.; Darling, S.B.; You, F. Perovskite photovoltaics: Life-cycle assessment of energy and environmental impacts. *Energy Environ. Sci.* **2015**, *8*, 1953–1968. [CrossRef]
15. Espinosa, N.; Serrano-Luján, L.; Urbina, A.; Krebs, F.C. Solution and vapour deposited lead perovskite solar cells: Ecotoxicity from a life cycle assessment perspective. *Sol. Energy Mater. Sol. Cells* **2015**, *137*, 303–310. [CrossRef]
16. Serrano-Lujan, L.; Espinosa, N.; Larsen-Olsen, T.T.; Abad, J.; Urbina, A.; Krebs, F.C. Tin- and lead-based perovskite solar cells under scrutiny: An Environmental perspective. *Adv. Energy Mater.* **2015**, *5*. [CrossRef]
17. Celik, I.; Song, Z.; Cimaroli, A.J.; Yan, Y.; Heben, M.J.; Apul, D. Life CYCLE assessment (LCA) of perovskite PV cells projected from lab to fab. *Sol. Energy Mater. Sol. Cells* **2016**. [CrossRef]

18. Albrecht, S.; Saliba, M.; Correa Baena, J.P.; Lang, F.; Kegelmann, L.; Mews, M.; Steier, L.; Abate, A.; Rappich, J.; Korte, L.; et al. Monolithic perovskite/silicon-heterojunction tandem solar cells processed at low temperature. *Energy Environ. Sci.* **2016**, *9*, 81–88. [CrossRef]
19. Bailie, C.D.; Christoforo, M.G.; Mailoa, J.P.; Bowring, A.R.; Unger, E.L.; Nguyen, W.H.; Burschka, J.; Pellet, N.; Lee, J.Z.; Gratzel, M.; et al. Semi-transparent perovskite solar cells for tandems with silicon and CIGS. *Energy Environ. Sci.* **2015**, *8*, 956–963. [CrossRef]
20. Fu, F.; Feurer, T.; Jäger, T.; Avancini, E.; Bissig, B.; Yoon, S.; Buecheler, S.; Tiwari, A.N. Low-temperature-processed efficient semi-transparent planar perovskite solar cells for bifacial and tandem applications. *Nat. Commun.* **2015**, *6*, 8932. [CrossRef] [PubMed]
21. Kranz, L.; Abate, A.; Feurer, T.; Fu, F.; Avancini, E.; Löckinger, J.; Reinhard, P.; Zakeeruddin, S.M.; Grätzel, M.; Buecheler, S.; et al. High-efficiency polycrystalline thin film tandem solar cells. *J. Phys. Chem. Lett.* **2015**, *6*, 2676–2681. [CrossRef] [PubMed]
22. Löper, P.; Moon, S.-J.; Martin de Nicolas, S.; Niesen, B.; Ledinsky, M.; Nicolay, S.; Bailat, J.; Yum, J.-H.; De Wolf, S.; Ballif, C. Organic-inorganic halide perovskite/crystalline silicon four-terminal tandem solar cells. *Phys. Chem. Chem. Phys.* **2015**, *17*, 1619–1629. [CrossRef] [PubMed]
23. Mailoa, J.P.; Bailie, C.D.; Johlin, E.C.; Hoke, E.T.; Akey, A.J.; Nguyen, W.H.; McGehee, M.D.; Buonassisi, T. A 2-terminal perovskite/silicon multijunction solar cell enabled by a silicon tunnel junction. *Appl. Phys. Lett.* **2015**, *106*, 121105. [CrossRef]
24. Werner, J.; Weng, C.-H.; Walter, A.; Fesquet, L.; Seif, J.P.; De Wolf, S.; Niesen, B.; Ballif, C. Efficient monolithic perovskite/silicon tandem solar cell with cell area >1 cm^2. *J. Phys. Chem. Lett.* **2016**, *7*, 161–166. [CrossRef] [PubMed]
25. Werner, J.; Walter, A.; Rucavado, E.; Moon, S.-J.; Sacchetto, D.; Rienaecker, M.; Peibst, R.; Brendel, R.; Niquille, X.; De Wolf, S.; et al. Zinc tin oxide as high-temperature stable recombination layer for mesoscopic perovskite/silicon monolithic tandem solar cells. *Appl. Phys. Lett.* **2016**, *109*, 233902. [CrossRef]
26. Almansouri, I.; Ho-Baillie, A.; Green, M.A. Ultimate efficiency limit of single-junction perovskite and dual-junction perovskite/silicon two-terminal devices. *Jpn. J. Appl. Phys.* **2015**, *54*, 08KD04. [CrossRef]
27. Espinosa, N.; Krebs, F.C. Life cycle analysis of organic tandem solar cells: When are they warranted? *Sol. Energy Mater. Sol. Cells* **2014**, *120*, 692–700. [CrossRef]
28. Monteiro Lunardi, M.; Wing Yi Ho-Baillie, A.; Alvarez-Gaitan, J.P.; Moore, S.; Corkish, R. A life cycle assessment of perovskite/silicon tandem solar cells. *Prog. Photovolt. Res. Appl.* **2017**. [CrossRef]
29. Frischknecht, R.; Itten, R.; Wyss, F.; Blanc, I.; Heath, G.; Raugei, M.; Sinha, P.; Wade, A. *Life Cycle Assessment of Future Photovoltaic Electricity Production from Residential-scale Systems Operated in Europe*; International Energy Agency (IEA) Photovoltaic Power Systems Program (PVPS) Task 12: Paris, France, 2015; ISBN 978-3-906042-30-5.
30. Rufer, D.; Braunschweig, A. Die bessere Ökobilanz von Solarstrom. *Umw. Perspekt.* **2013**, *4*, 9–13.
31. Frischknecht, R.; Itten, R.; Sinha, P.; de Wild-Scholten, M.; Zhang, J.; Fthenakis, V.; Kim, H.C.; Raugei, M.; Stucki, M. *Life Cycle Inventories and Life Cycle Assessments of Photovoltaic Systems*; IEA PVPS Task 12, Subtask 2.0, LCA Report IEA-PVPS 12 April 2015; International Energy Agency Photovoltaic Power Systems Program: Paris, France, 2015.
32. Frischknecht, R.; Heath, G.; Raugei, M.; Sinha, P.; de Wild-Scholten, M.; Fthenakis, V.; Kim, H.C.; Alsema, E.; Held, M. *Methodology Guidelines on Life Cycle Assessment of Photovoltaic Electricity*, 3rd ed.; IEA PVPS Task 12; International Energy Agency Photovoltaic Power Systems Programme: Paris, France, 2016.
33. *Ecoinvent Centre Ecoinvent Data v3.3*; Swiss Centre for Life Cycle Inventories: Zürich, Switzerland, 2016.
34. Baldassarri, C.; Shehabi, A.; Asdrubali, F.; Masanet, E. Energy and emissions analysis of next generation electrochromic devices. *Life Cycle Environ. Ecol. Impact Anal. Sol. Technol.* **2016**, *156*, 170–181. [CrossRef]
35. Classen, M.; Althaus, H.-J.; Blaser, S.; Scharnhorst, W.; Tuchschmid, M.; Jungbluth, N.; Faist Emmenegger, M. *Life Cycle Inventories of Metals*; Swiss Centre for Life Cycle Inventories: Dübendorf, Switzerland, 2009.
36. Hischier, R.; Classen, M.; Lehmann, M.; Scharnhorst, W. *Life Cycle Inventories of Electric and Electronic EquipmentProduction, Use & Disposal*; Swiss Centre for Life Cycle Inventories: St. Gallen, Switzerland, 2007.
37. Hauschild, M.; Goedkoop, M.; Guinée, J.; Heijungs, R.; Huijbregts, M.A.J.; Jolliet, O.; Margni, M.; De Schryver, A. *Recommendations for LIFE Cycle Impact Assessment in the European context—Based on Existing Environmental Impact Assessment Models and Factors*; European Commission—DG Joint Research Centre, JRC, Institute for Environment and Sustainability (IES): Brussels, Belgium, 2011.

38. Intergovernmental Panel on Climate Change (IPCC). Contribution of working group I to the fifth assessment report of the Intergovernmental Panel on Climate Change. In *Climate Change 2013: The Physical Science Basis*; Cambridge University Press: Cambridge, UK, 2013.
39. Frischknecht, R.; Jungbluth, N.; Althaus, H.-J.; Doka, G.; Dones, R.; Heck, T.; Hellweg, S.; Hischier, R.; Nemecek, T.; Rebitzer, G.; et al. *Overview and Methodology*; Swiss Centre for Life Cycle Inventories: Dübendorf, Switzerland, 2007.
40. *PRé Consultants SimaPro 8.3 Software*; PRé Consultants BV: Amersfoort, The Netherlands, 2016.
41. Trube, J.; Metz, A.; Fischer, M.; Hsu, A.; Julsrud, S.; Chang, T.; Tjahjono, B. *International Technology Roadmap for Photovoltaic (ITRPV) 2016 Results*, 8th ed.; VDMA Photovoltaic Equipment: Frankfurt, Germany, 2017.
42. Burschka, J.; Pellet, N.; Moon, S.-J.; Humphry-Baker, R.; Gao, P.; Nazeeruddin, M.K.; Graetzel, M. Sequential deposition as a route to high-performance perovskite-sensitized solar cells. *Nature* **2013**, *499*, 316–319. [CrossRef] [PubMed]
43. Yang, W.S.; Noh, J.H.; Jeon, N.J.; Kim, Y.C.; Ryu, S.; Seo, J.; Seok, S.I. High-performance photovoltaic perovskite layers fabricated through intramolecular exchange. *Science* **2015**, *348*, 1234. [CrossRef] [PubMed]
44. Kaizuka, I.; Kurihara, R.; Matsukawa, H.; Masson, G.; Nowak, S.; Brunisholz, M.; Orlandi, S. *Trends 2015 in Photovoltaic Applications—Survey Report of Selected IEA Countries between 1992 and 2014*; Task 1; International Energy Agency Photovoltaic Power Systems Program: Paris, France, 2015.
45. Moon, S.J.; Yum, J.H.; Löfgren, L.; Walter, A.; Sansonnens, L.; Benkhaira, M.; Nicolay, S.; Bailat, J.; Ballif, C. Laser-Scribing Patterning for the Production of Organometallic Halide Perovskite Solar Modules. *IEEE J. Photovolt.* **2015**, *5*, 1087–1092. [CrossRef]
46. Espinosa, N.; García-Valverde, R.; Urbina, A.; Krebs, F.C. A life cycle analysis of polymer solar cell modules prepared using roll-to-roll methods under ambient conditions. *Solar Energy Mater. Solar Cells* **2011**, *95*, 1293–1302. [CrossRef]
47. Braun, M. *Incorporated Slot Die Coater—High Precision Functional Liquid Film Coating*; M. Braun Incorporated: Stratham, NH, USA, 2017.
48. Jungbluth, N.; Stucki, M.; Flury, K.; Frischknecht, R.; Buesser, S. *Life Cycle Inventories of Photovoltaics*; ESU-Services Ltd.: Uster, Switzerland, 2012.
49. Rekinger, M.; Theologitis, I.-T.; Masson, G.; Latour, M.; Biancardi, D.; Roesch, A.; Concas, G.; Basso, P. *Connecting the Sun—Solar Photovoltaics on the Road to Large-Scale Grid Integration*; European Photovoltaic Industry Association (EPIA): Brussels, Belgium, 2012.
50. Candelise, C.; Winskel, M.; Gross, R. Implications for CdTe and CIGS technologies production costs of indium and tellurium scarcity. *Prog. Photovolt. Res. Appl.* **2012**, *20*, 816–831. [CrossRef]
51. Arvidsson, R.; Kushnir, D.; Molander, S.; Sandén, B.A. Energy and resource use assessment of graphene as a substitute for indium tin oxide in transparent electrodes. *J. Clean. Prod.* **2016**, *132*, 289–297. [CrossRef]
52. Zimmermann, Y.-S.; Niewersch, C.; Lenz, M.; Kül, Z.Z.; Corvini, P.F.-X.; Schäffer, A.; Wintgens, T. Recycling of indium from CIGS photovoltaic cells: Potential of combining acid-resistant nanofiltration with liquid–liquid extraction. *Environ. Sci. Technol.* **2014**, *48*, 13412–13418. [CrossRef] [PubMed]
53. Hailegnaw, B.; Kirmayer, S.; Edri, E.; Hodes, G.; Cahen, D. Rain on methylammonium lead iodide based perovskites: Possible environmental effects of perovskite solar cells. *J. Phys. Chem. Lett.* **2015**, *6*, 1543–1547. [CrossRef] [PubMed]
54. Babayigit, A.; Duy Thanh, D.; Ethirajan, A.; Manca, J.; Muller, M.; Boyen, H.-G.; Conings, B. Assessing the toxicity of Pb- and Sn-based perovskite solar cells in model organism Danio rerio. *Sci. Rep.* **2016**, *6*, 18721. [CrossRef] [PubMed]
55. Babayigit, A.; Ethirajan, A.; Muller, M.; Conings, B. Toxicity of organometal halide perovskite solar cells. *Nat. Mater.* **2016**, *15*, 247–251. [CrossRef] [PubMed]
56. Gutschner, M.; Nowak, S.; Ruoss, D.; Toggweiler, P.; Schoen, T. *Potential for Building Integrated Photovoltaics*; IEA PVPS Task 7-4; NET Nowak Energy & Technology Ltd.: Ursen, Switzerland, 2002.